Supplemental data. Collakova et al. (2008). *Arabidopsis* 10-Formyl Tetrahydrofolate Deformylases Are Essential for Photorespiration.

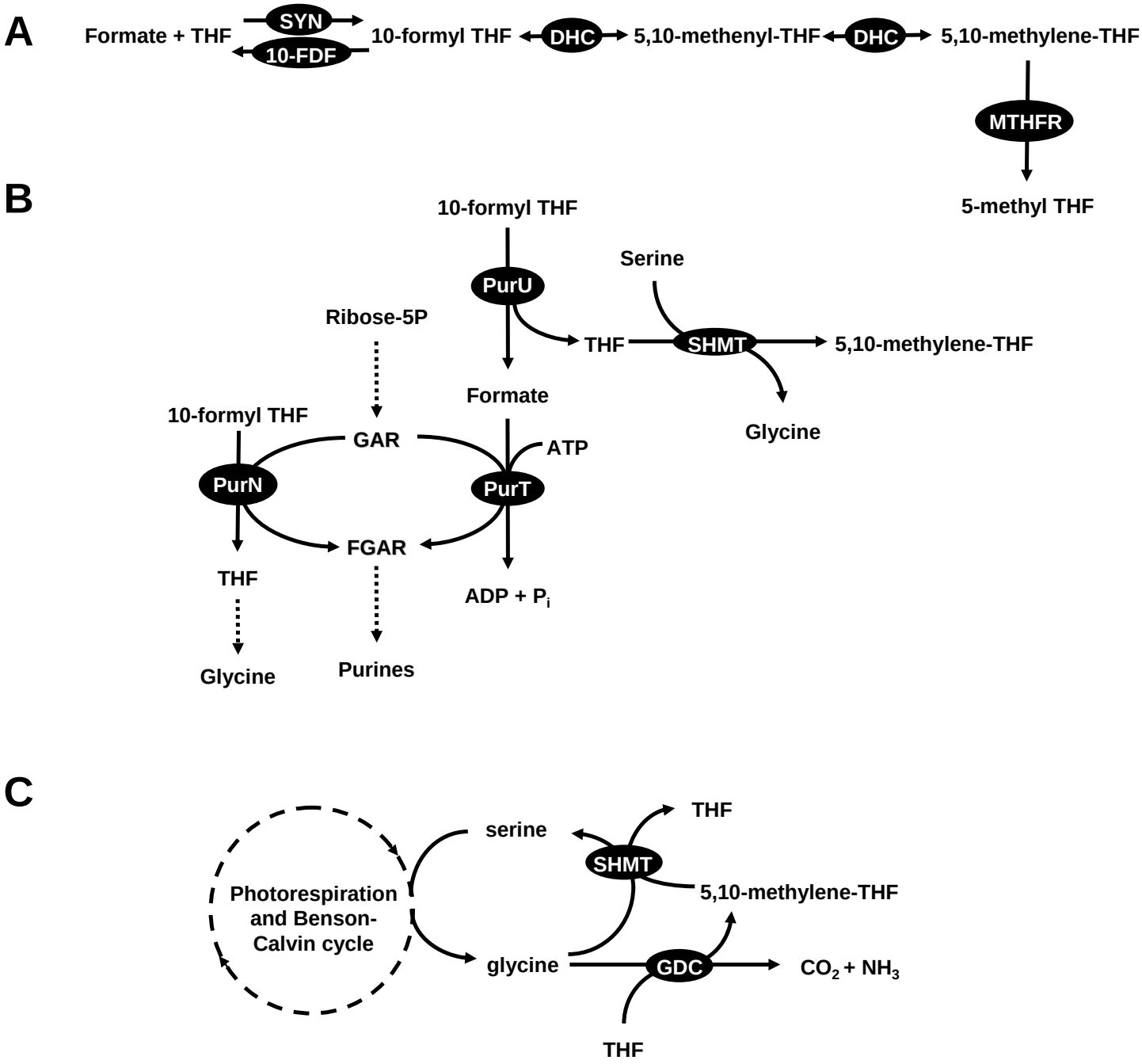

Supplemental Figure 1. Pathways involving folate interconversions. (A) Folate species inter-conversions and enzymes involved; **(B)** Purine and glycine biosyntheses in *E. coli*. PurN, PurU, and PurT are involved in de- or trans-formylation reactions in purine biosynthesis. PurN catalyzes the transfer of the formyl group from 10-formyl THF and PurT the attachment of formate produced by PurU, respectively, to glycinamide-5'-phosphoribo-nucleotide (GAR) to form N-formylglycinamide-5'-phosphoribonucleotide (FGAR). Tetrahydrofolate (THF) released by PurN and PurU is used for glycine synthesis by serine hydroxymethyl-transferase (SHMT); **(C)** Photorespiratory glycine to serine conversion involves folate-dependent glycine decarboxylase (GDC) and SHMT. Abbreviations: DHC, 5,10-methylene THF dehydrogenase/ 5,10-methenyl THF cyclohydrolase; 10-FDF, 10-formyl THF deformylase (PurU in *E. coli*); MTHFR, 5,10-methylene THF reductase; SYN, 10-formyl THF synthetase

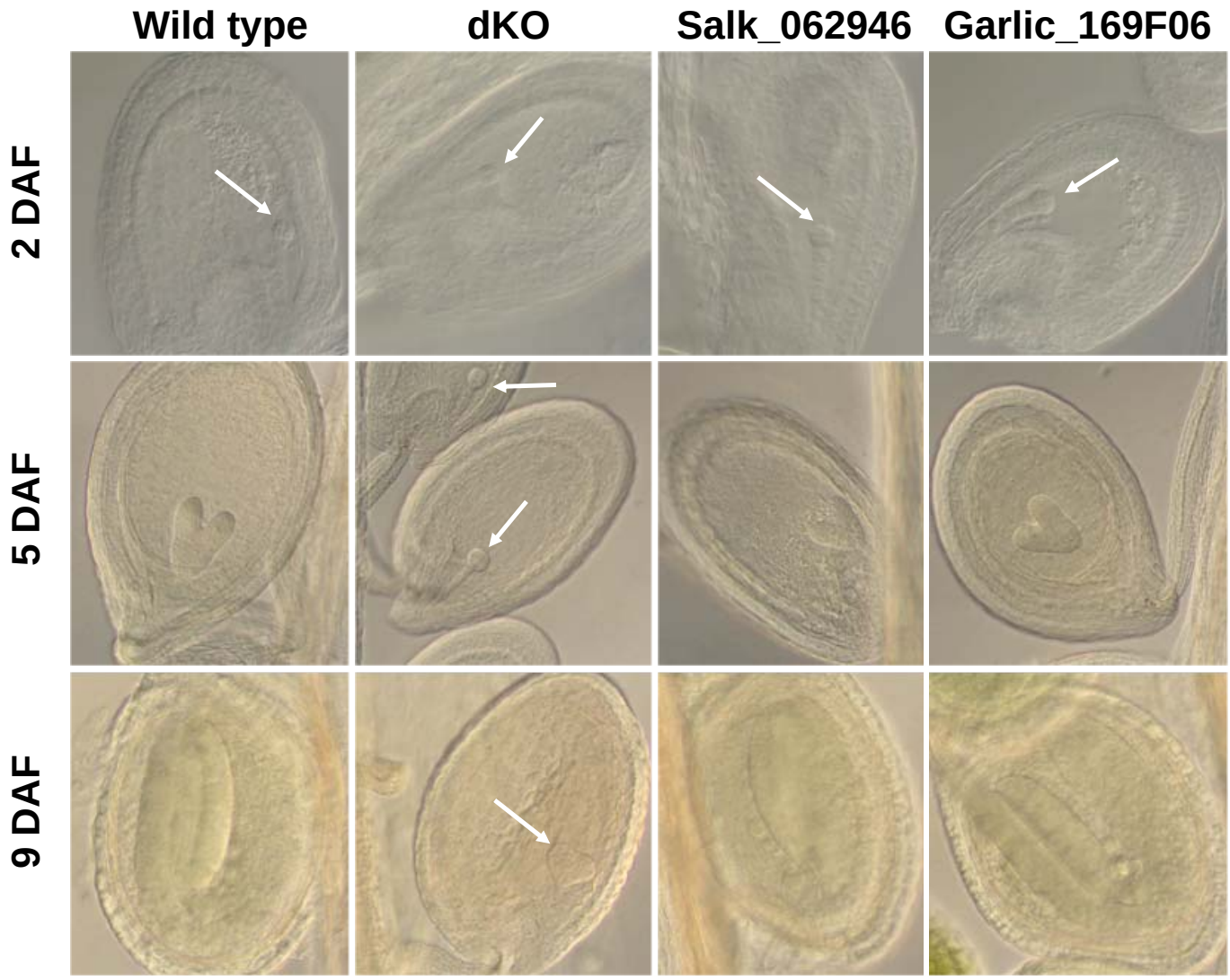

Supplemental Figure 2. Parallel comparison of embryo development in wild type, dKO, and corresponding single homozygous mutant lines. Plants were grown in ambient air at 12-hour photoperiod and flowers marked to follow seed development. Siliques were harvested at indicated days after flowering (DAF), cleared in Hoyer solution and mounted for Nomarski (2 DAF) or bright field (5 and 9 DAF) microscopy. Development of dKO embryos is severely delayed, while the embryos of single homozygous mutants (Salk_062946 and Garlic_169F06) develop normally. Unlike dKO, at 5 DAF both wild type and single mutant embryos reach heart stage. At 9 DAF they are fully developed as bent cotyledon embryos. White arrows facilitate visualization of globular (and triangular for dKO 5 DAF) stages of embryo development.

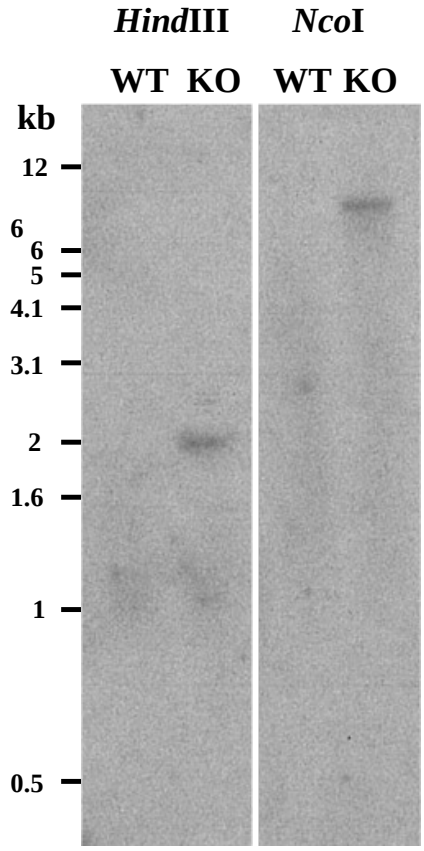

Supplemental Figure 3. Southern blot analysis of wild type and Garlic 169F06 single mutant plants. Genomic DNA was isolated from two grams of leaves pooled from 20 plants of Garlic_169F06 T-DNA insertion mutants (KO) or the corresponding wild type (WT) siblings obtained from the segregating plants. Genomic DNA (5 µg per lane) was digested with *Hind*III, which cuts the T-DNA 311 bp downstream of the probe or *Nco*I, which cuts the T-DNA 3.8 kb downstream of the probe. The probe was a 436-bp fragment of the *bar* gene located within the T-DNA and amplified using the forward 5'-CATCGTCAACCACTACATCG-3' and reverse 5'-GAAGTCCAGCTGCCAGAAAC-3' primers. Only single hybridizing bands were observed in the mutant plants, establishing that the T-DNA is inserted only at the At5g47435 locus.

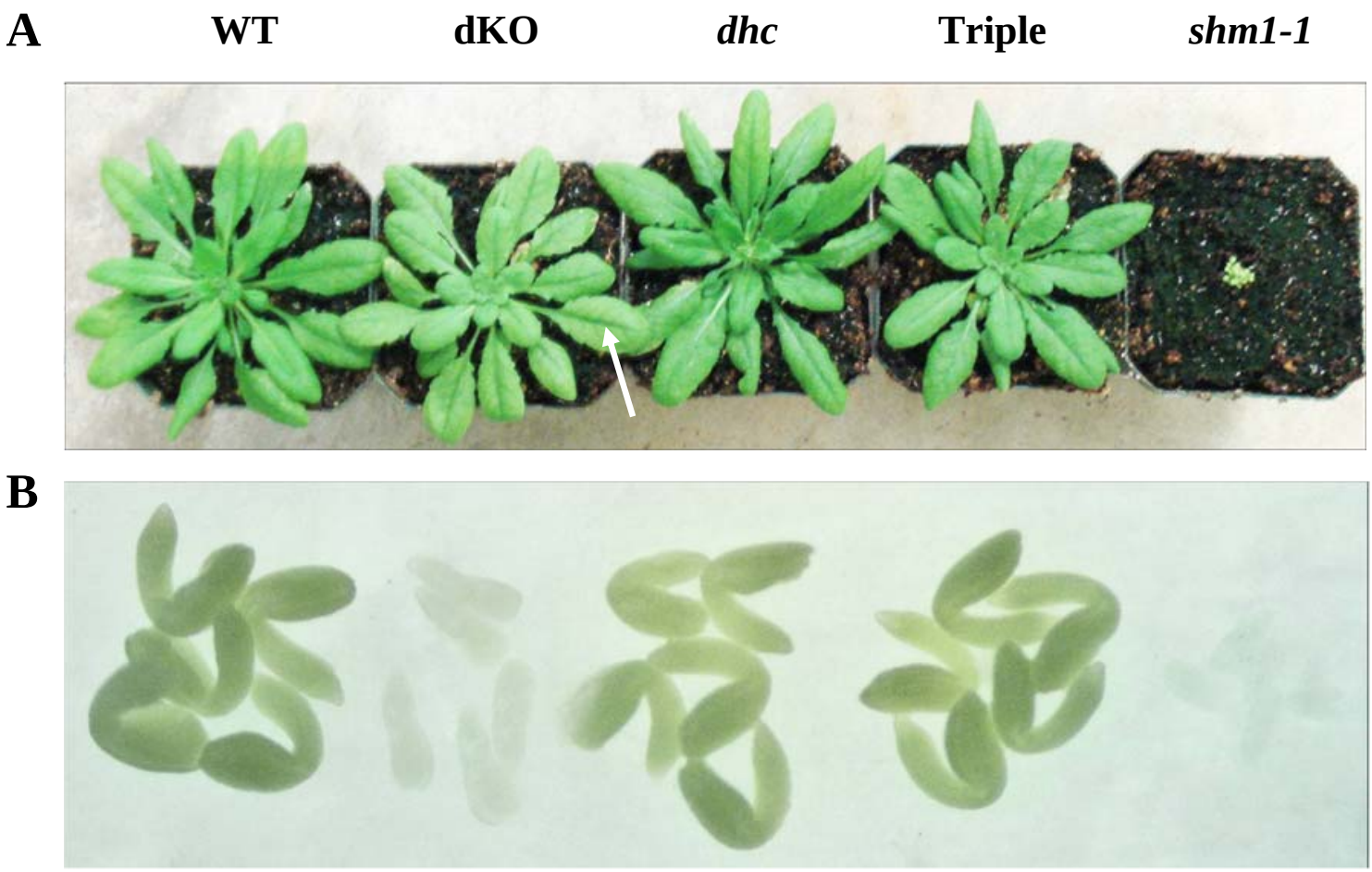

Supplemental Figure 4. Parallel comparison of phenotypes in wild type and mutant plants. (A) Plants (wild type, dKO, *shm1-1*, *dhc*, and triple homozygous mutant) were grown in ambient air at 12-hour photoperiod for six weeks. **(B)** Dissected 13-day-old embryos, for which plants were pre-grown at high CO_2 conditions prior to exposure to ambient air to obtain flowering *shm1-1* mutant for embryo dissection. Only dKO and *shm1-1* mutants show visible phenotypes. Please note the dark green veins and paler leaves in the dKO mutant (white arrow in panel A). The *dhc* and triple (homozygous dKO X *dhc*) mutants are indistinguishable from the wild type based on visual comparison and they produce normal viable embryos.

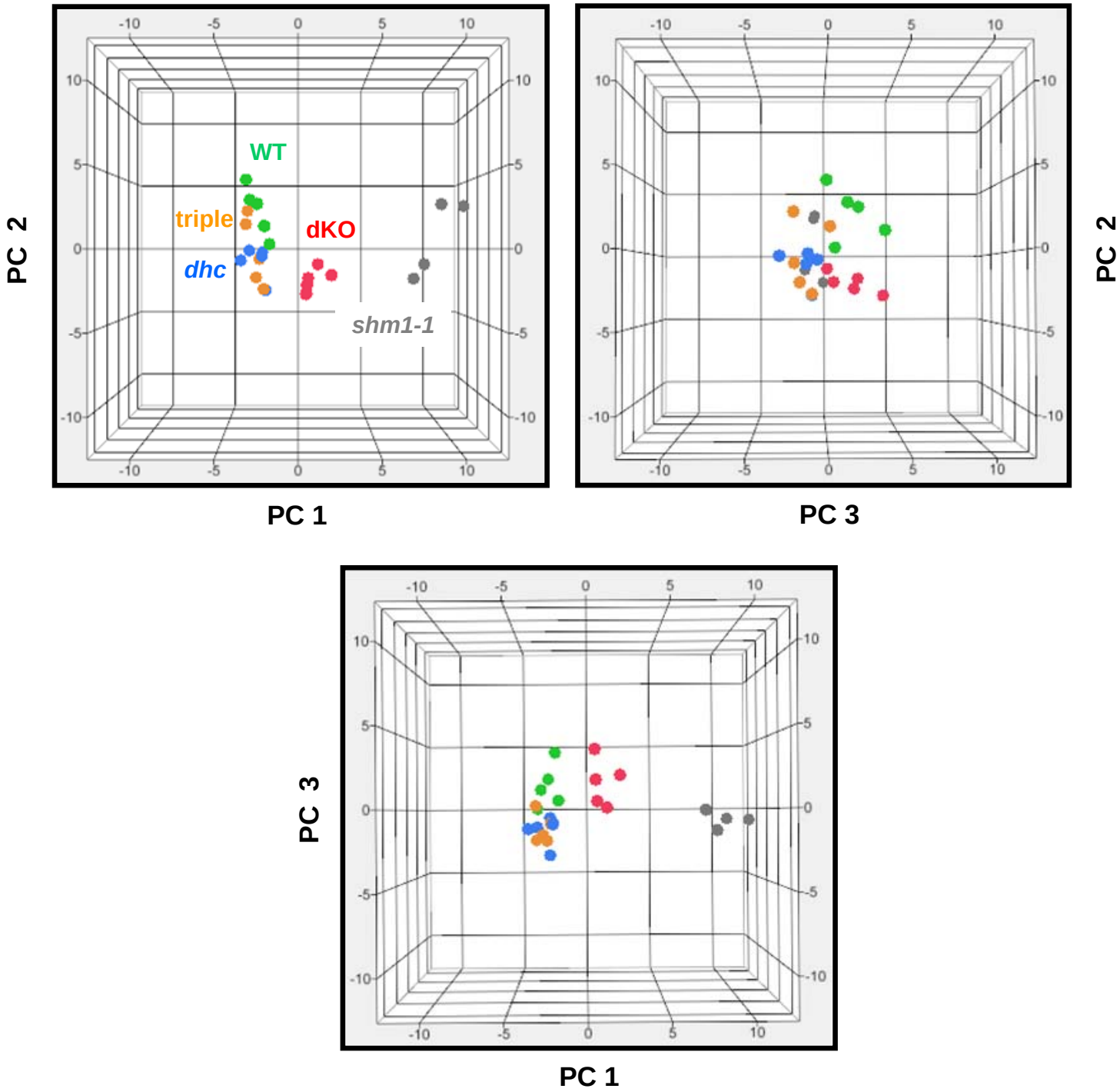

Supplemental Figure 5. Principal Component Analysis (PCA) on correlations of major metabolites in wild type and mutant plants. Plants (wild type, dKO, *shm1-1*, *dhc*, and triple homozygous mutant) were grown in ambient air at 12-hour photoperiod for two weeks after pre-growth at high CO_2 for three weeks. Fifty two metabolites were analyzed by GC-MS (4 -5 biological replicates) and their relative levels were normalized for dry weight and recovery. PCA analysis was performed by using JMP statistical software. Only first three components and their combinations are shown, as they include 61% of the variance among the samples. dKO and *shm1-1* mutants are well separated from the wild type and other mutants based on Principal Component (PC) 1, suggesting that their metabolite profiles are different from the wild type. In this context, metabolite profiles of the *dhc* and triple homozygous mutants were similar to the wild type. None of the genotypes was separated based on PC 2 and 3, indicating that these components include biological variation within the genotypes rather than variance among the genotypes.

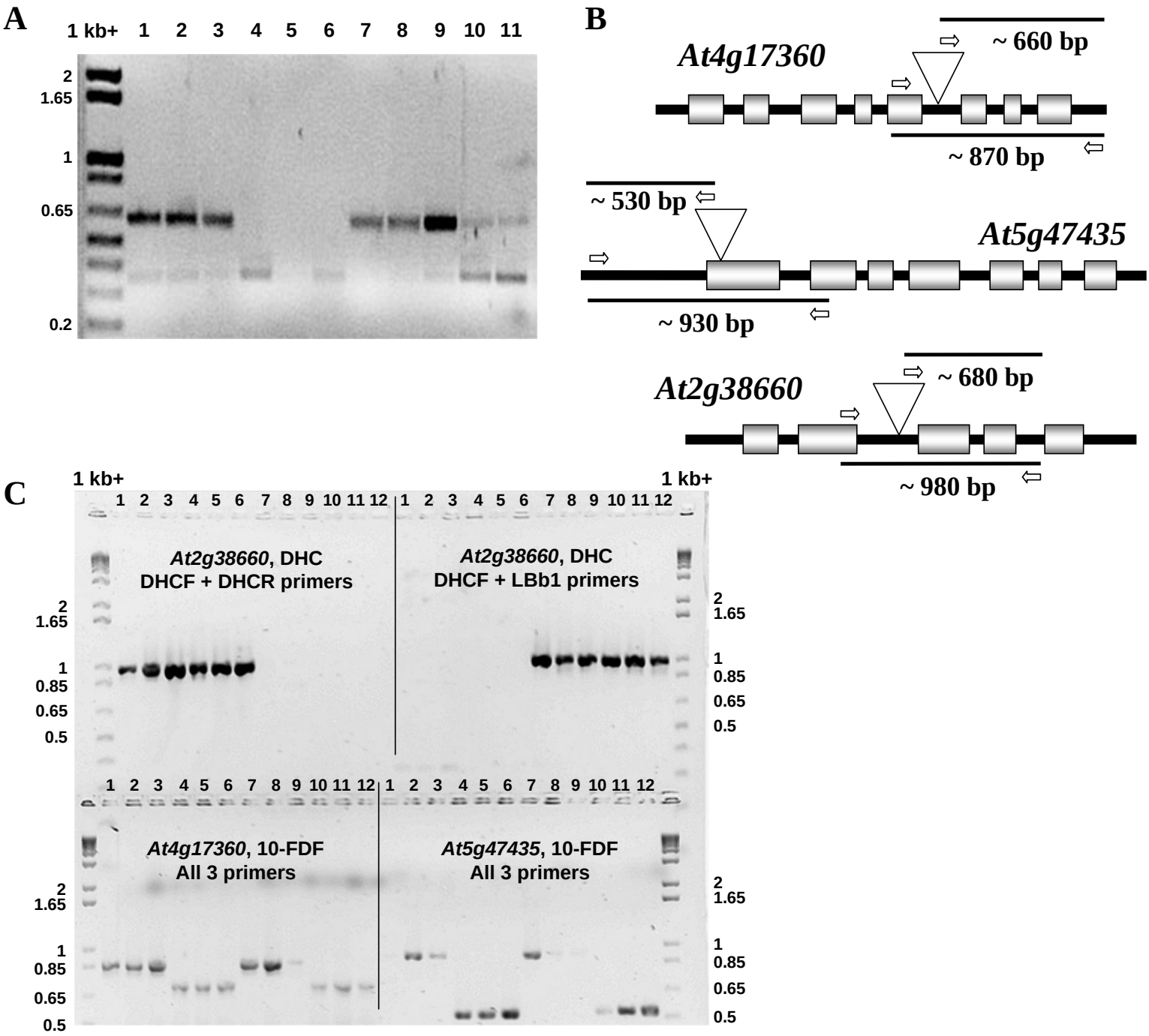

Supplemental Figure 6. RT-PCR and genotyping results. (A) RT-PCR of two different DHC mutant lines and the corresponding wild type plants. mRNA was reverse transcribed and cDNA generated using an oligo-dT primer. Primers DHCF1 and DHCR1 used in PCR should produce an amplicon at 544 bp in the mutant background. Lanes 1 to 3: wild type from segregating Salk_143478; lanes 4 to 6: homozygous Salk_143478; lanes 7 to 9: wild type from segregating Salk_142776; Lanes 10 and 11: homozygous Salk_142776. **(B)** Predicted fragment pattern for genotyping three representative wild type and mutant plants presented in panel C. Genes: exons are represented by gray rectangles, while introns or untranslated regions by thick black lines. Primers are depicted as white arrows and T-DNA insertion as triangles. **(C)** Genotyping of wild type (lanes 1 to 3); homozygous dKO - Garlic_169F06 X Salk_062946 (lanes 4 to 6); homozygous *dhc* mutant - Salk_143478 (lanes 7 to 9); and triple homozygous mutant - Garlic_169F06 X Salk_062946 X Salk_143478 (lanes 10 to 12). The fragment patterns for *At4g17360* and *At5g47435* were consistent with the predictions, but the PCR with DHCF and T-DNA specific LBb1 primers for *At2g38660* gave a larger product (~ 1 kb as opposed to ~ 680 bp) probably due to tandem T-DNA insertions. Therefore, to distinguish between wild type and T-DNA-containing lines, two separate PCR reactions were performed to amplify the wild type- and T-DNA-specific fragments.